Supplemental Information

Supplemental Data

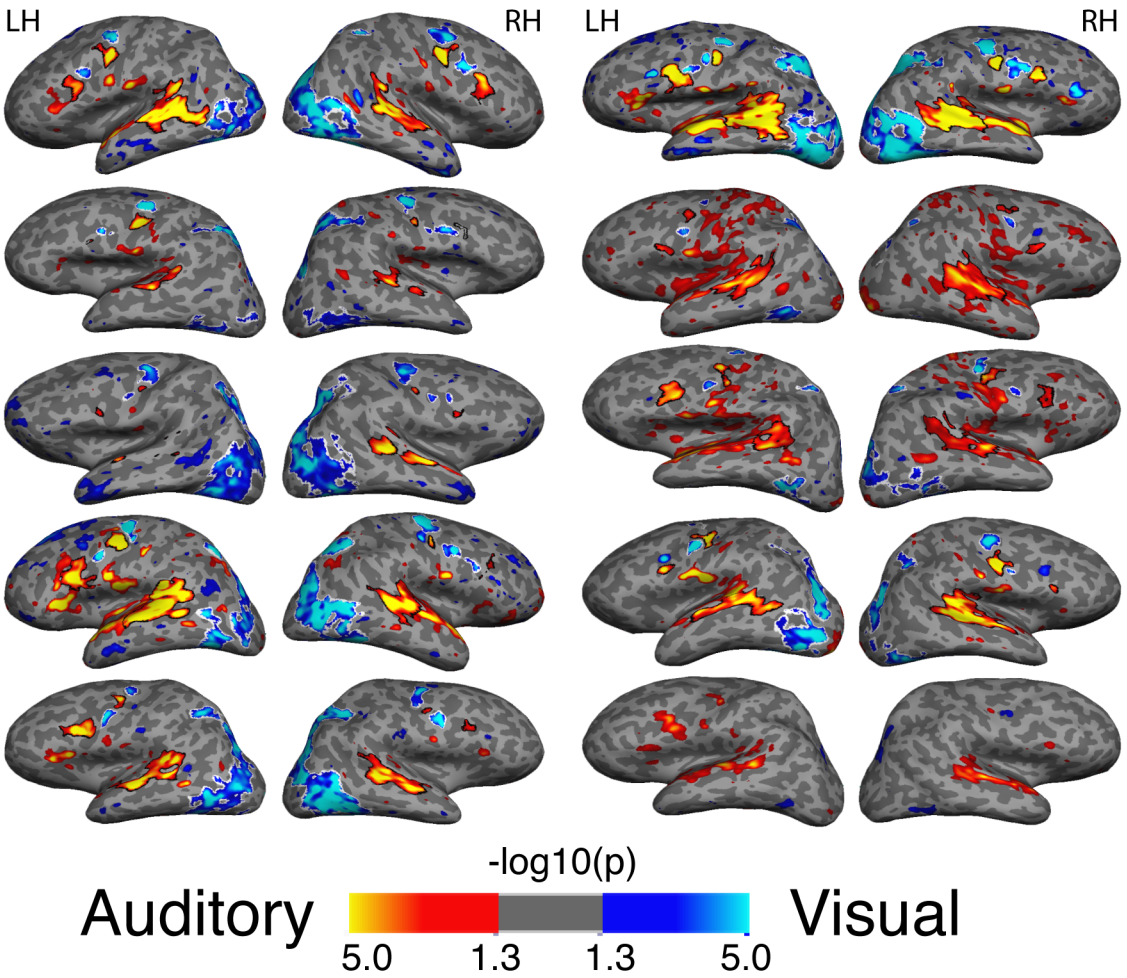

Figure S1, Related to Figure 2: Individual subject maps for all 10 subjects. Black and white outlines represent ROI definitions for auditory- and visual-biased ROIs, respectively.

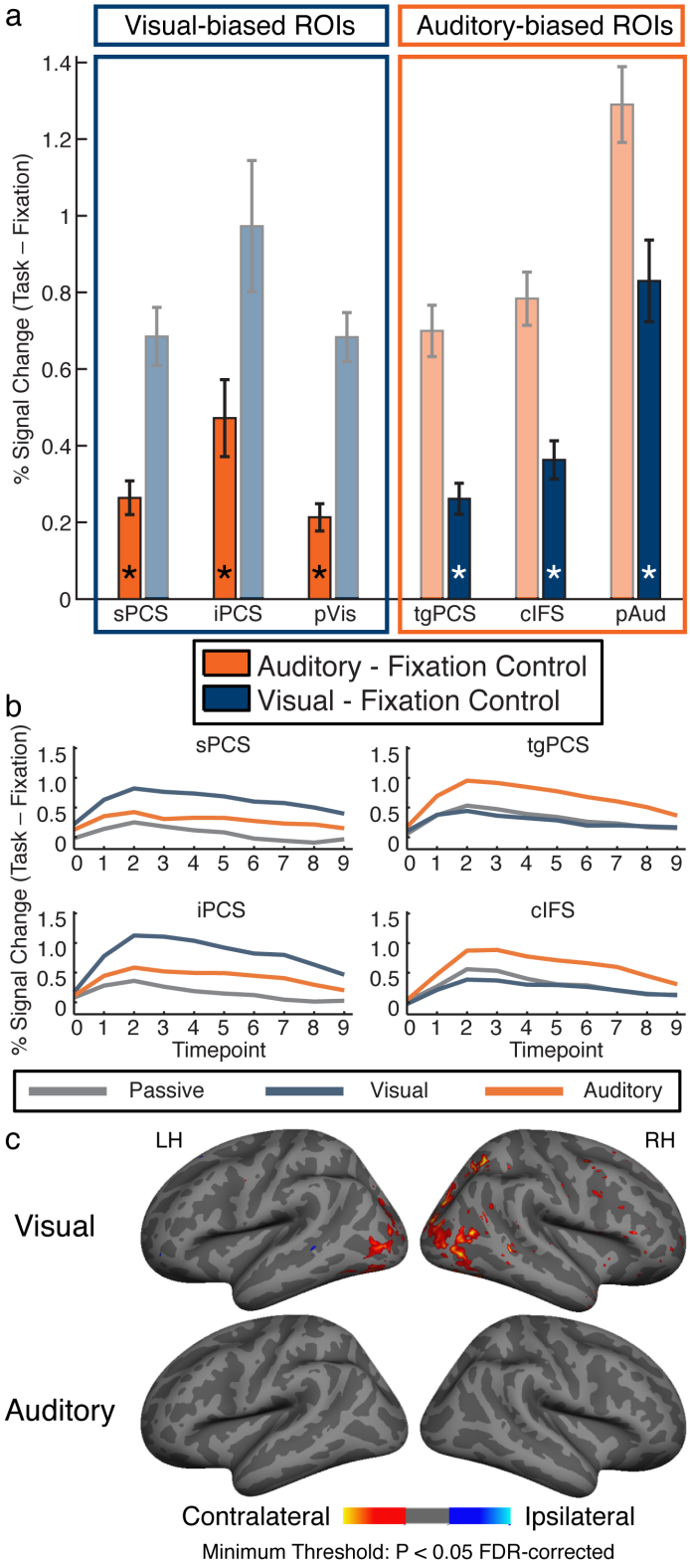

Figure S2, Related to Figure 2: (a) Average (n = 9) percent signal change relative to a fixation baseline control for auditory spatial attention and visual spatial attention conditions. * represents $p < 0.05$, Holm-Bonferroni corrected. **(b)** Average (n = 9) percent signal change timecourses of auditory, visual, and passive blocks relative to fixation baseline. **(c)** Group average (n = 10, since no ROIs required) statistical maps of contralateral bias within visual attention blocks (top) and auditory attention blocks (bottom) from Experiment 1. Contralateral bias is defined as "attend left" greater than "attend right" in the right hemisphere and "attend right" greater than "attend left" in the left hemisphere.

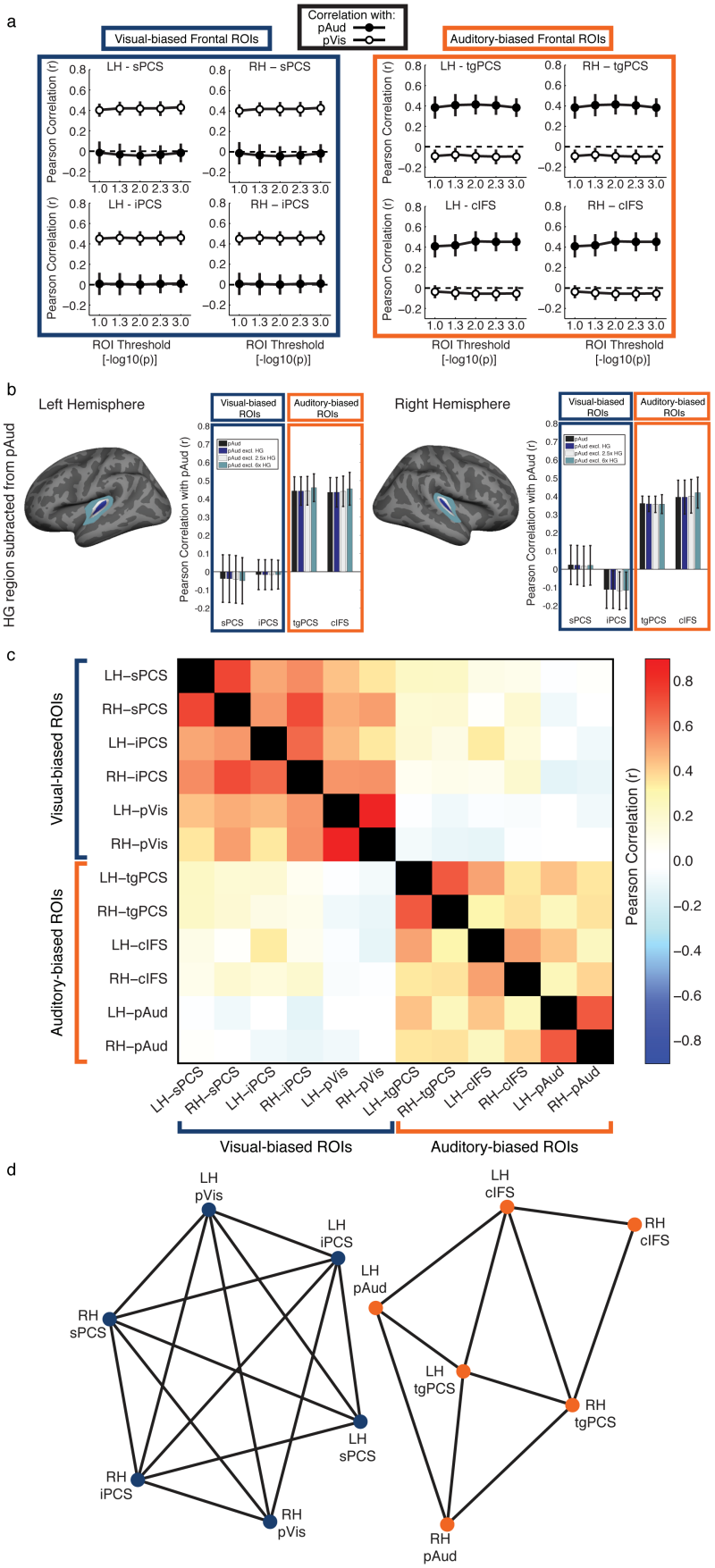
a
Visual-biased Frontal ROIs
Correlation with:
pAud
pVis
Auditory-biased Frontal ROIs
LH - sPCS
RH – sPCS
LH - iPCS
RH – iPCS
LH - tgPCS
RH – tgPCS
LH - cIFS
RH – cIFS
Pearson Correlation (r)
ROI Threshold [-log10(p)]
b
Left Hemisphere
Right Hemisphere
HG region subtracted from pAud
Visual-biased ROIs
Auditory-biased ROIs
Pearson Correlation with pAud (r)
pAud
pAud excl. HG
pAud excl. 2.5x HG
pAud excl. 6x HG
sPCS
iPCS
tgPCS
cIFS
c
Visual-biased ROIs
Auditory-biased ROIs
LH–sPCS
RH–sPCS
LH–iPCS
RH–iPCS
LH–pVis
RH–pVis
LH–tgPCS
RH–tgPCS
LH–cIFS
RH–cIFS
LH–pAud
RH–pAud
Pearson Correlation (r)
d
LH pVis
LH iPCS
RH sPCS
LH sPCS
RH iPCS
RH pVis
LH cIFS
RH cIFS
LH pAud
LH tgPCS
RH tgPCS
RH pAud

Figure S3, Related to Figure 3: (a) Effect of statistical threshold for ROI definition on intrinsic functional connectivity from Experiment 2. *Post hoc* analysis to assess if the intrinsic functional connectivity findings were biased by the statistical threshold selected for ROI definition ($p < 0.05$). Within subjects, each ROI was defined using 5 statistical thresholds ($p < 0.10$ to $p < 0.001$). Lines show mean within-hemisphere correlations ($n = 7$) between frontal ROIs and posterior ROIs (pVis and pAud); error bars reflect s.e.m. Two subjects were excluded because a subset of ROIs could not be defined at the highest statistical threshold. No change in intrinsic functional connectivity was observed across statistical thresholds. **(b)** Effect of excluding anatomical Heschl's Gyrus (HG) from the pAud ROI on intrinsic functional connectivity from Experiment 2. HG was defined using the Desikan-Killiany atlas and dilated on the cortical surface to 2.5 and 6 times the number of surface vertices. Bars show mean within-hemisphere correlations ($n = 9$) between frontal ROIs and pAud ROIs with 4 levels of HG exclusion. The pAud bars (black) are identical to the pAud bars in Figure 3. Error bars reflect s.e.m. **(c)** Correlation matrix for all ROIs defined in Experiment 1 illustrating that the predicted pattern continued across hemispheres and throughout the two networks. **(d)** Graph structure of thresholded rsFC connections ($p < 0.05$ Holm-Bonferroni corrected). The Kamada-Kawai spring embedded algorithm was used to determine graph structure.

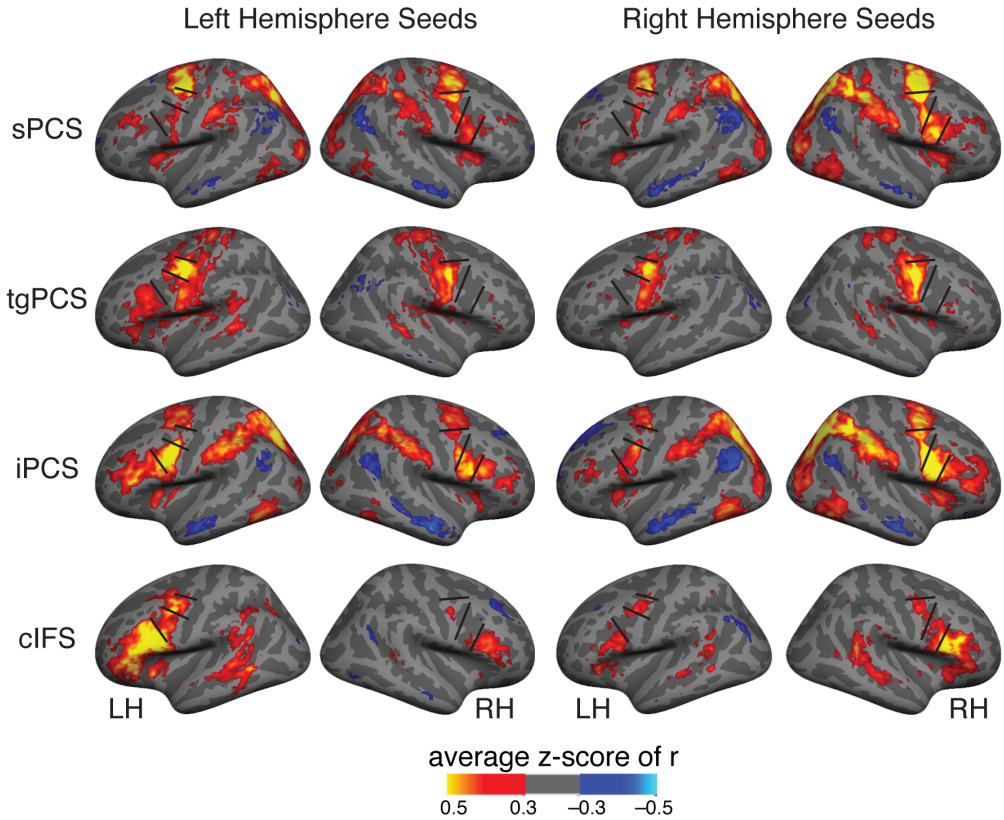

Figure S4 Related to Figure 3: Resting-state functional connectivity maps based on each frontal ROI, independently by hemisphere. Maps represent the group average ($n = 9$) of the z-scores of the correlations between each of 8 seed region and all surface vertices on each hemisphere of the brain. The black lines were added to serve as anatomical reference points.

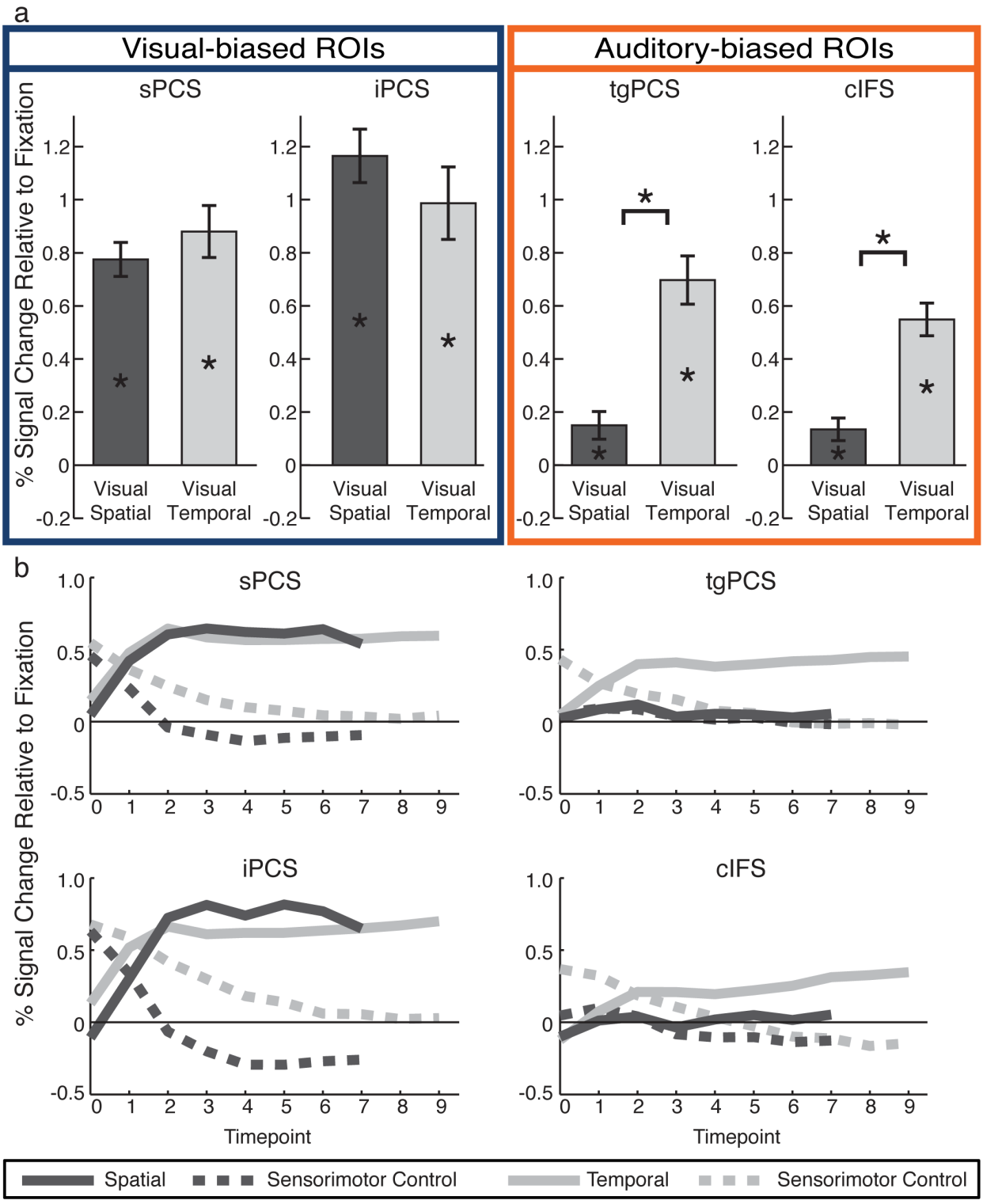

Figure S5, Related to Figure 4: (a) Average percent signal change (n = 9) relative to a fixation baseline control for the visual spatial and temporal short-term memory conditions in Experiment 3. * represents $p < 0.05$, Holm-Bonferroni corrected. (b) Average percent signal change timecourses of visual temporal task condition, sensorimotor control for the visual temporal condition, visual spatial task condition, and sensorimotor control for the visual spatial condition, each compared to fixation baseline.

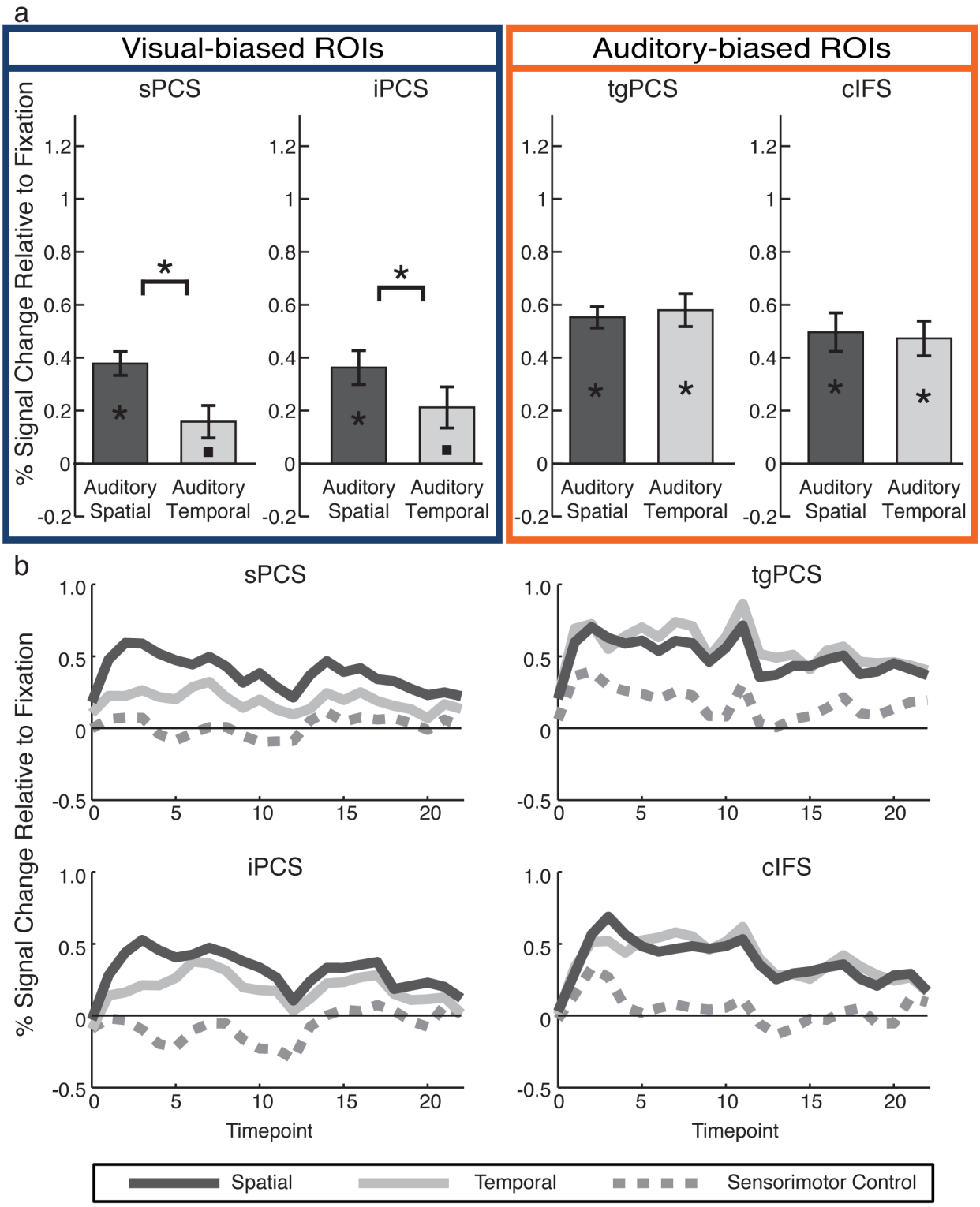

Figure S6, Related to Figure 5: (a) Average percent signal change (n = 9) relative to a fixation baseline control for auditory spatial and temporal short-term memory conditions in Experiment 4. * represents $p < 0.05$, and square represents $p < 0.06$, Holm-Bonferroni corrected. (b) Average percent signal change timecourses of auditory spatial, auditory temporal, and sensorimotor control conditions, each compared to fixation baseline.

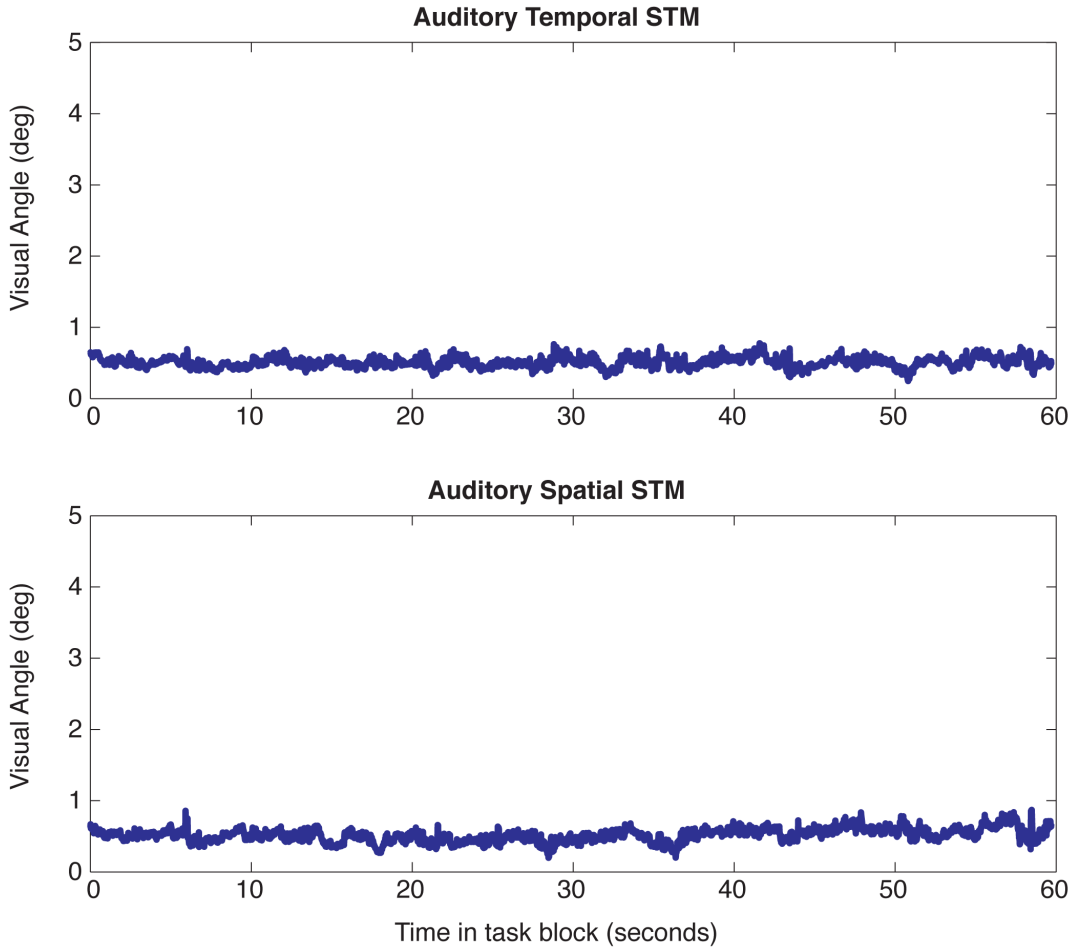

Figure S7, Related to Figure 5: Root mean square distance from fixation along the x-axis showing the average fixation deviation across blocks and subjects. A repeated-measures ANOVA indicated no difference between the Auditory Temporal and Auditory Spatial STM conditions when evaluating distance from fixation, $F(1,6) = 0.447$, $p = 0.53$.

Supplemental Experimental Procedures

Resting state functional connectivity analysis in Experiment 2

The resting-state data underwent additional processing using Matlab to reduce artifacts that could lead to spurious functional connectivity. Following the preprocessing described above, the data underwent multiple regression with nuisance regressors including the average white matter signal, average signal from the ventricular regions of interest, whole brain signal averaged across the whole brain, and 12 motion regressors (6 motion parameters from Freesurfer motion correction and their 6 temporal derivatives). We then calculated the framewise displacement (Power et al., 2012) for each timepoint and implemented impute-first scrubbing (Carp, 2013), where timepoints with framewise displacement greater than 0.5 mm were replaced with imputed values using nearest neighbor interpolation. We then applied a band-pass filter with $0.01 < f < 0.08$ Hz (Chao-Gan and Yu-Feng, 2010). After filtering, we removed the timepoints with high framewise displacement that were previously replaced with imputed values. We then calculated the average timecourse within each of the 12 ROIs defined in Experiment 1 for each subject. The Pearson's correlation coefficients were calculated for each posterior ROI (pVis and pAud) with each frontal ROI (sPCS, tgPCS, iPCS, and cIFS) within each hemisphere. Prior to averaging correlation data across subjects, the correlation coefficients for each subject were transformed using the Fisher r-to-z transform to mitigate the issue of non-additivity of correlation coefficients. Group-level significance of within-participant correlations was tested using t-tests on the z-values. Each of the 16 correlations was tested for significance compared to no correlation. For each frontal ROI, we compared its correlation with each of the two posterior ROIs. All correlation values reported are the average Pearson correlations computed using Fisher's z-to-r transformation on the group average. All t-tests were then corrected for multiple comparisons using the Holm-Bonferroni method using the R software package (http://CRAN.R-project.org).

Hierarchical clustering was conducted using the Bioinformatics toolbox in Matlab 7.5 (similar to analysis conducted by Dosenbach et al, 2007). We used a distance measure of (1 – r) and a common average linkage method (UPGMA). Cluster tree branch points were validated using 1000 bootstraps, each created by

randomly sampling (with replacement) 9 correlation matrices from the pool of 9 subjects. The 9 correlation matrices were combined by converting to z-scores, averaging, and converting back to r, in order to create a distance (1 – r) matrix. The cluster branches were verified by calculating the percentage of bootstrap trees containing a subtree that matched a subtree in the original cluster tree, in that both subtrees contained exactly the same ROIs, independent of the ordering of ROIs within the subtree.

To confirm our findings from the hierarchical analysis, we applied graph theory to our resting state functional connectivity data using Matlab. Pairwise BOLD correlations (functional connections) were extracted for each combination and shown in Figure S3c. In our unweighted, binary graphs, the 12 ROIs served as nodes and edges were defined by positive correlations with $p < 0.05$ (Holm-Bonferroni corrected) between a given pair of ROIs. Graphs were visualized using Pajek (http://vlado.fmf.uni-lj.si/pub/networks/pajek/) and the Kamada-Kawai spring embedded algorithm was used to determine the spatial organization of the graphs.

Eye tracking analysis

In Experiment 1 and Experiment 4, 9 of the participants were eye-tracked in the scanner using the EyeLink 1000 system from SR Research; technical issues prevented proper eyetracking in the remaining 2 subjects, who were both experienced subjects with a proven ability to hold fixation both outside of the scanner and during other tasks in the scanner. In Experiment 4, all included participants made saccadic eye movements (> 2°) in less than 7% of trials, with no difference in the number of saccadic eye movements between the spatial and temporal task ($t_6 = 0.35$, $p = 0.74$).

An additional analysis of eye position (similar to Jack et al., 2006) also revealed no differences between the auditory spatial and temporal conditions. Here, a continuous trace of horizontal and vertical eye positions were sampled at 50 Hz and analyzed using Matlab. Blinks were detected using pupil size and vertical position and removed from further analysis. The eye traces shown in Figure S7 illustrate the distance from fixation along the horizontal axis (azimuth), determined by taking the root mean square difference of the processed horizontal traces from their median value for the trial. This was averaged across trials to create an average for each participant for each task condition; these participant averages were then averaged at each time point to

create Figure S7. For statistical analysis of the root mean square distance, we calculated the distance from the trial median (including horizontal and vertical position) for each time point in the trial. We then found the average root mean square distance for each trial. The average root mean square distance for each of the 8–10 trials per condition for each participant were entered into a repeated measures ANOVA with participant as a repeated factor. The repeated-measures ANOVA indicated no difference between the Auditory Temporal and Auditory Spatial STM conditions when evaluating distance from fixation, $F(1,6) = 0.447$, $p = 0.53$.

Supplemental References

Carp, J. (2013). Optimizing the order of operations for movement scrubbing: Comment on Power et al. NeuroImage 76, 436-8.

Chao-Gan, Y., and Yu-Feng, Z. (2010). DPARSF: A MATLAB Toolbox for "Pipeline" Data Analysis of Resting-State fMRI. Front Syst Neurosci 4, 13.

Dosenbach, N. U., Fair, D. A., Miezin, F. M., Cohen, A. L., Wenger, K. K., et al. (2007). Distinct brain networks for adaptive and stable task control in humans. Proceedings of the National Academy of Sciences 104(26), 11073-11078.

Jack, A. I., Shulman, G. L., Snyder, A. Z., McAvoy, M., & Corbetta, M. (2006). Separate modulations of human V1 associated with spatial attention and task structure. Neuron 51(1), 135–147.

Power, J., Barnes, K., Snyder, A., Schlaggar, B., and Petersen, S. (2012). Spurious but systematic correlations in functional connectivity MRI networks arise from subject motion. NeuroImage 59 (3), 2142-54.